

Momentum Distribution Techniques

Conservation of momentum during the annihilation process is the reason for the fact that the annihilation radiation contains information on the electron momentum distribution at the annihilation site. This can be used for the study of the electron structure in solids and for the investigation of defects. There are two basic techniques studying the momentum distribution: Doppler-broadening spectroscopy and angular correlation of annihilation radiation.

1. Principle of the Momentum Distribution Techniques

As a result of momentum conservation during the annihilation process, the momentum of the electron–positron pair, \mathbf{p} , is transferred to the photon pair. The momentum component p_z in the propagation direction z of the γ -rays results in a Doppler shift ΔE of the annihilation energy of 511 keV, which amounts approximately to

$$\Delta E = p_z c/2. \quad (1)$$

Since numerous annihilation events are measured to give the complete Doppler spectrum, the energy line of the annihilation is broadened due to the individual Doppler shifts in both directions, $\pm z$. This effect is utilized in Doppler-broadening spectroscopy, which is described in Sect. 2.3.2.

The momentum components $p_{x,y}$ perpendicular to the propagation direction lead to angular deviations $\Theta_{x,y}$ of the collinearity of the annihilation γ -rays according to

$$\Theta_{x,y} = \frac{p_{x,y}}{m_0 c} \quad (2)$$

m_0 is the rest mass of the electron. These equations hold for small angles. $\Theta_{x,y}$ can be registered simultaneously in both x and y directions by a coincidence measurement using position-sensitive detection of the γ -quanta. This technique is known as the angular correlation of annihilation radiation.

The momentum conservation during the annihilation process gives a tool to study the momentum distribution of electrons in the solid. The momentum of the positron after thermalization is significantly smaller than that of most electrons. The reason is the Pauli principle and the resulting distribution of the electron momenta up to the Fermi momentum. Although the positron is also a Fermi particle, it can thermalize, because there is no more than one positron in the sample at a given time. This allows the probing of the electron distribution in the electron structure in the momentum space. The effect of the localization of positrons in lattice defects enables such a study, not only in the bulk, but also for open-volume defects. Due to the limited energy resolution of Doppler-broadening

spectroscopy, electron structure investigations are carried out mainly by angular correlation of annihilation radiation.

In the case of localization of positrons in open-volume defects, the fraction of valence electrons taking part in the annihilation process increases compared with that of core electrons. Because the momentum of valence electrons is significantly lower, the momentum distribution of annihilating electrons shifts to smaller values. This means a smaller angular deviation for ACAR and a smaller Doppler broadening for DOBS. The curve of defect-rich material is thus higher and narrower than that of defect-free reference material, when both curves are normalized to equal area.

Typical Doppler-broadening spectra measured for as-grown and plastically deformed GaAs are compared in Fig. 1 with the resolution function measured as the 514-keV γ -line of ^{85}Sr . The comparison of the measured GaAs curves to this reference γ -line illustrates the effect of Doppler broadening of the annihilation line. Typical values of the FWHM of the ^{85}Sr curve are between 1 and 2 keV.

As an example of the application of momentum techniques for defect investigations, the Doppler spectra of as-grown and plastically deformed GaAs are compared in Fig.1. If the Doppler curves are normalized to equal area, the curve of the deformed sample is higher due to the occurrence of vacancy-type defects. This effect can be used to get quantitative information about these defects.

Similar investigations providing the kind and concentration of defects in the sample are in principle also possible with angular correlation of annihilation radiation. However, 2D-ACAR is very time consuming for defect investigations

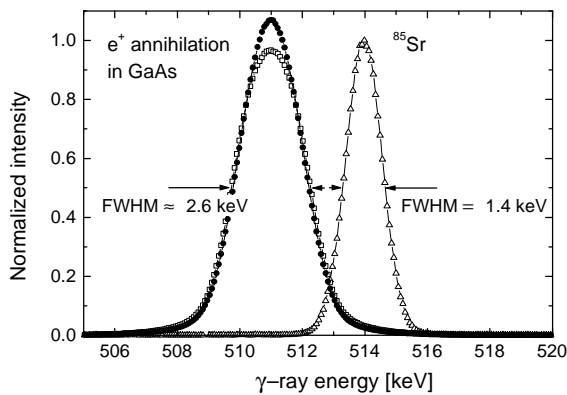


Fig. 1. Doppler-broadening spectra of as-grown (\square) and plastically deformed (\bullet) gallium arsenide (Hübner et al. 1997b). The Doppler lines of GaAs are broadened compared with the reference line of ^{85}Sr at 514 keV. The full width at half maximum (FWHM) of this reference line characterizes the Gaussian resolution function of the spectrometer. The intensity is normalized to the peak height of the strontium curve (\triangle). The lines are drawn to guide the eye.

and cannot be carried out with positron lifetime spectroscopy at the same time. ACAR has thus rarely been used for defect studies in semiconductors.

An advantage of the momentum techniques is their sensitivity to the chemical environment of the annihilation site, which is higher compared with positron lifetime spectroscopy. This is because the momentum distribution information is more influenced by the chemical surroundings than the electron density, which is the basis of the positron lifetime technique.

2. Measurement of Annihilation-Line Doppler Broadening

The Doppler-broadening technique requires an energy-dispersive system. Compared with the angular correlation technique, a compact and relatively simple setup is possible and, thus, such spectrometers are used in almost all positron laboratories.

2.1 Experimental Setup

The energy broadening of the annihilation line described above is measured by a high-resolution energy-dispersive detector system (Fig. 2). Liquid-nitrogen-cooled pure Ge crystals of high efficiency (about 20 %) are used. Under the applied high voltage of several kV, the annihilation photons cause a charge separation that is converted by a preamplifier into an electrical pulse. Its amplitude is a measure of the photon energy and can be registered after main amplification in a multi-channel analyzer (MCA). A digital peak-stabilizing system as part of the MCA allows the long-term collection of several million counts. The time of the

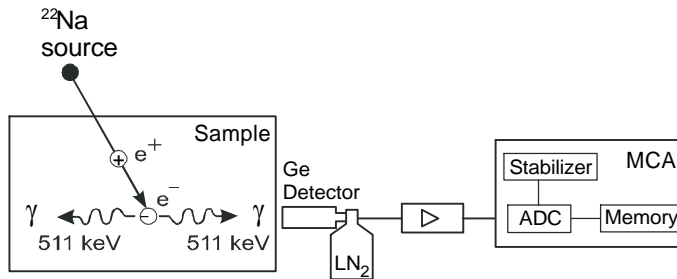


Fig. 2. Experimental arrangement of Doppler-broadening spectroscopy. The energy distribution of the annihilation line is measured with a liquid nitrogen (LN_2) cooled germanium detector. The signal of the pure-Ge detector is processed by a preamplifier integrated in the detector. A spectroscopy amplifier provides the necessary pulses for the subsequent digitally stabilized analog-digital converter (ADC). The event is stored in the memory of the multi-channel analyzer (MCA).

measurement is comparable to the collection time of a positron lifetime spectrum. Both techniques can easily be performed at the same time because the Ge detector should be separated sufficiently from the sample in order to avoid pile-up effects in the detector system.

The background can be drastically reduced by the application of the Doppler-broadening coincidence technique, which registers both γ -quanta. This technique is especially important for the measurement of the high-momentum part as far as 9 keV away from the center of the annihilation line. The experimental setup for this technique is shown in Fig. 3. The second annihilation γ -quantum, being almost collinear to the primarily monitored quantum, can be detected in a second Ge detector. Alternatively, a cheaper scintillator/photomultiplier detector may be used. The main advantage of the system with two Ge detectors is the improvement of the energy resolution, ideally by a factor of $\sqrt{2}$ (MacDonald et al. 1978).

The coincident γ -quantum serves to reduce the background arising mainly from the 1.27-MeV γ -quanta of the β^+ -decay in the source. The background can be suppressed by at least two orders of magnitude in this way. The first experimental realizations of such a coincidence setup were reported by Lynn et al. (1977), MacDonald et al. (1978), and Troev et al. (1979). The first application of this technique to semiconductors was given by Iwase et al. (1985b), who studied the lateral distribution of grown-in defects in an InP wafer. A major step forward in the evaluation of coincidence spectra was the combination with theoretical

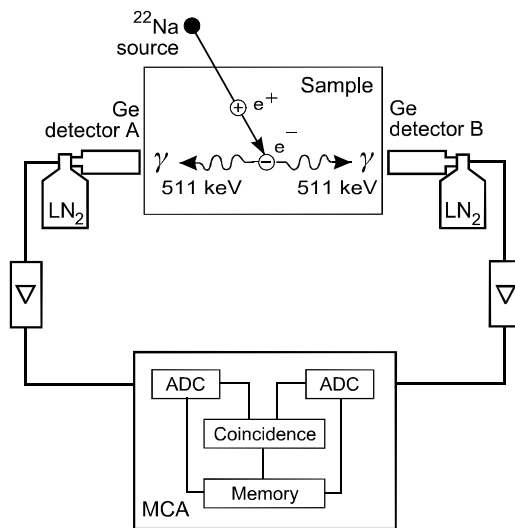


Fig. 3. Coincidence setup for the measurement of background-reduced Doppler-broadening spectra. Two liquid nitrogen (LN_2) cooled germanium detectors are used for the registration of the collinear coincidence γ -quanta (ADC—analogue-digital converter, MCA—multi-channel analyzer).

calculations of the high-momentum part of the annihilation line (Alatalo et al. 1995, 1996; Asoka-Kumar 1997; Asoka-Kumar et al. 1996).

The result is a two-dimensional array of counting rates, where the dimensions represent the energy scales of the respective detectors. An example is shown in Fig. 4. A coincidence spectrum of both Ge detectors is obtained as the intensity profile along the diagonal from the upper left to lower right of the measured array. This diagonal profile can be explained by momentum conservation during the annihilation process. The increase in the annihilation γ -ray energy in one detector according to the Doppler shift (Fig. 2) leads to a simultaneous reduction of the γ -ray energy in the second detector, i.e. the sum of the annihilation γ -ray energies remains constant at 1022 keV. The second diagonal is a measure of the resolution of the system. The profiles parallel to the axes at the energy of 511 keV are also coincident spectra. The second detector provides in this case only the gate pulse for the detection of the γ -quanta. Although these spectra also have a reduced background, they are still asymmetrical (closed squares in Fig. 4 b). Such spectra are usually also obtained if, instead of a second Ge detector, a scintillator is used. A background reduction of better than one order of magnitude is still possible with a scintillation detector with an optimized setup. The diagonal coincidence spectrum is almost symmetrical and has the improved energy resolution mentioned above. This becomes obvious in Fig. b, where the improved peak-to-

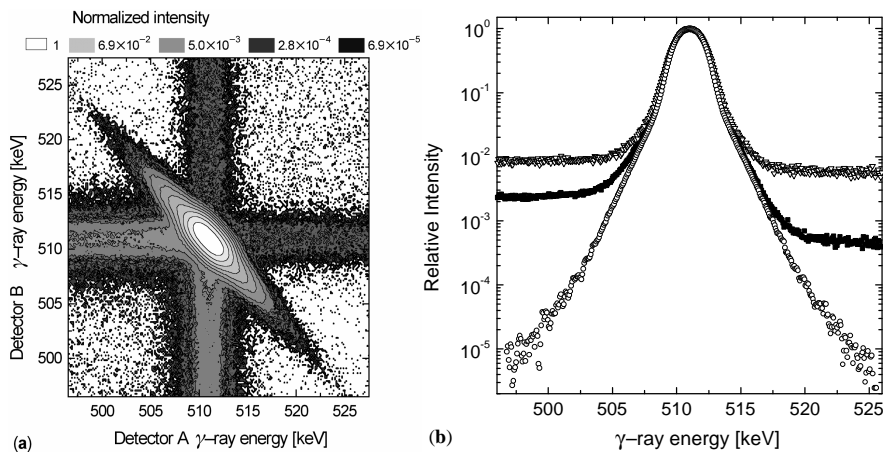


Fig. 4. Doppler-broadening coincidence spectra of zinc-doped gallium arsenide (Gebauer and Krause-Rehberg 1998). **(a)** Two-dimensional array of coincident annihilation events. The vertical and horizontal axes are the γ -ray energies of two germanium detectors arranged according to Fig.. The gray value represents the counting rate normalized to peak maximum. **(b)** Demonstration of the background reduction. The Doppler-broadening spectrum (∇) was measured conventionally (Fig. 2) with one Ge detector. The coincidence spectra were obtained from (a) as intensity profiles parallel to the horizontal axis at an energy of 511 keV (\blacksquare) and diagonal (\circ).

background ratio of 10^{-5} and the better resolution are visible.

2.2 Data Treatment

The effect of positron trapping in defects on the Doppler-broadening spectrum $N_D = f(E)$ is demonstrated in Fig. 5. The quantitative evaluation can be carried out with specific line shape parameters. The S parameter¹ is defined as the area of the central low-momentum part of the spectrum, A_s , divided by the area below the whole curve A_0 after background subtraction,

$$S = \frac{A_s}{A_0}, \quad A_s = \int_{E_0 - E_s}^{E_0 + E_s} N_D dE \quad (3)$$

The W parameter² is taken in a high-momentum region far from the center, as indicated in Fig. 5. It is calculated as the area of the curve in a fixed energy interval, A_w , divided by A_0 ,

$$W = \frac{A_w}{A_0}, \quad A_w = \int_{E_1}^{E_2} N_D dE. \quad (4)$$

The interval limits are chosen symmetrically around the energy of $E_0 = 511$ keV for the calculation of the S parameter, $E_0 \pm E_s$. The energy limits E_1 and E_2 for the W parameter must be defined in such a way as to have no correlation effects with the S parameter. These chosen limits are kept constant for all spectra to be compared. For the determination of the S parameter, the curves of a defect-rich sample and a sample free of positron traps are plotted in Fig. 5 normalized to equal area. The S parameter limits should be taken as the intersection points of both curves to obtain the largest sensitivity for a defect-induced change in the line shape. Often, these limits were simply taken to give an S parameter of 0.5 for defect-free material. This means that the determination of W must start at a limit significantly separated from the intersection points of the curves. The limits were set to (511 ± 0.8) keV for the determination of S and to $(511 + 2.76)$ and $(511 + 4)$ keV for W in the example of Fig. 5. The ratio of the S parameters for the plastically deformed and the GaAs reference sample was found to be 1.0695. The corresponding ratio of the W parameters was 0.7726.

The background correction is often performed as the subtraction of a straight line. More sophisticated treatments use a realistic background distribution modeled by a non-linear function. This function takes into account that the background at a given γ -ray energy is proportional to the sum of annihilation

¹ "Shape" parameter; recently also called the valence annihilation parameter.

² "Wing" or core annihilation parameter.

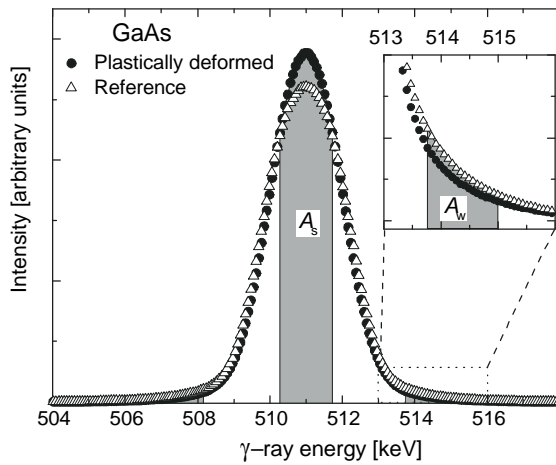


Fig. 5. Doppler-broadening spectra of as-grown zinc-doped gallium arsenide showing no positron trapping (reference) compared with plastically deformed GaAs (Hübner et al. 1997b). The line shape parameters S and W are determined by the indicated areas A_s and A_w divided by the area below the whole curve. The curves are normalized to equal area.

events with higher energies. Despite such a background reduction, the Doppler curve remains slightly unsymmetrical. The calculation of the W parameter is, therefore, frequently carried out only in the high-energy wing of the Doppler curve. High-quality Doppler-broadening spectra are obtained by the coincidence technique, preferably with a setup using two Ge detectors. In this case, the W parameters can be taken on both sides of the curve.

The line shape parameters S and W are commonly normalized to their respective bulk values, S_b and W_b . The advantage of such a normalization is that, independent of the chosen limits for the determination of S and W from the Doppler spectrum, the obtained values can be compared. This does not hold for the comparison of values measured with different spectrometers. The reason is the dependence of the normalized line shape parameters on the resolution of the spectrometer (Fig. 6). The deviations of the S parameter resulting from differing spectrometer resolutions are much larger than the statistical errors. Resolutions ranging from 1.2 to 2.2 eV were reported. Fig. 6 clearly demonstrates that S parameter values reported in the literature and obtained with different spectrometers cannot be directly compared.

A further method for the quantification of the annihilation line shape is the calculation of so-called RID curves³ (Coleman 1979). For the calculation, the difference of the normalized Doppler curves and its running integral is

³ Running integrals of difference curves.

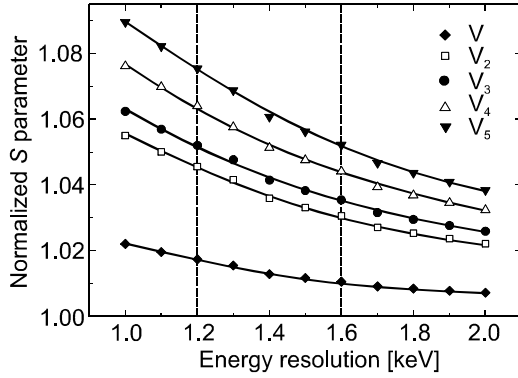


Fig. 6. Dependence of the S parameter on the energy resolution of the Doppler-broadening spectrometer. This dependence was obtained from theoretical spectra calculated for different vacancy clusters in silicon (Hakala et al. 1998). It was convolved by Gaussians of different full widths at half maximum simulating the energy resolution (Eichler 1997). The S parameters were each normalized to the respective bulk value convolved by the same Gaussian. The dashed lines indicate the resolution limits of frequently used spectrometers.

determined. Information on the type and density of defects may be obtained from the resulting curve. Difficulties arise when more than one defect type contributes significantly to the spectrum. No broad applications of this method are known. Another possibility of defect identification and quantification is the evaluation of difference or ratio curves. A reference spectrum, e.g. a Gaussian function or the spectrum from the defect-free bulk, may be used to reveal hidden details in the Doppler-broadening spectra in order to obtain a fingerprint of the defect structure.

The W parameter is more sensitive to the chemical surrounding of the annihilation site than the S parameter, because the core electrons having a high momentum are contributing mainly in the region of large energy deviations from the annihilation energy of 511 keV.

Both the S and W parameters are sensitive to the concentration and kind of the defect. In order to obtain the defect concentration, one has to presume the defect type, i.e. the defect-related parameters S_d and W_d . A new parameter, R , can be defined, which depends only on the defect type, but not on the concentration (Mantl and Triftshäuser 1978),

$$R = \frac{|S - S_b|}{|W - W_b|} = \frac{|S_d - S_b|}{|W_d - W_b|}. \quad (5)$$

Instead of the numerical calculation of R from (5), the graphic presentation of $S = S(W)$ gives R for one defect type as the slope of the straight line through (W_b, S_b) and (W_d, S_d) . Such S versus W plots (Clement et al. 1996; Liskay et al. 1994) for differently treated samples, e.g. after annealing, may show the presence

of more than one defect type (for more details on the R parameter and S versus W plots).

It is possible to calculate the high-momentum part of the annihilation line. Such theoretical curves are compared with those experimentally obtained in order to get structural and chemical information. The procedure was first applied to vacancies in InP (Alatalo et al. 1995). The isolated phosphorus and indium vacancies were distinguished from each other by the magnitude of the core-electron annihilation. Furthermore, the zinc decoration of phosphorus vacancies in InP:Zn was identified. First-principles calculations have been presented to calculate the momentum distribution of the annihilating electron–positron pair (e.g. Gilgien et al. 1994; Hakala et al. 1998; Tang et al. 1997). Complete angular correlation of annihilation radiation spectra can be obtained and from them, by integration and convolution, whole Doppler-broadening spectra.

3. Angular Correlation of Annihilation Radiation

The momentum components $p_{x,y}$ perpendicular to the propagation direction are related to the deviations $\Theta_{x,y}$ of the collinearity of the annihilation γ -rays according to (2). Since the annihilation γ -quanta are emitted simultaneously, $\Theta_{x,y}$ can be measured in a coincidence arrangement by position-sensitive detectors. The coincidence counting rate N_c is given as the integral of the momentum distribution of the annihilating positron–electron pair, $\sigma = \sigma(p_x, p_y, p_z)$, versus the momentum component p_z in the propagation direction of the annihilation radiation,

$$N_c(\Theta_x, \Theta_y) = A_c \int_{-\infty}^{\infty} \sigma(\Theta_x m_0 c, \Theta_y m_0 c, p_z) dp_z. \quad (6)$$

A_c is a constant. As described above, the electron–positron momentum distribution in z direction gives the Doppler shift of the annihilation γ -quanta. The integration in (6) is due to the lack of energy-dispersive position-sensitive detectors, i.e. every measured point represents all events of the corresponding Doppler spectrum. As the momentum distribution is recorded in two dimensions, this technique is referred to as 2D-ACAR.

The first ACAR measurements in one dimension were realized with Geiger counters by Behringer and Montgomery (1942). A position-sensitive detection can be realized in the simplest way in one dimension (1D-ACAR) by the mechanical movement of a long scintillation detector (Hautojärvi and Vehanen 1979; Mijnaerends 1979). The integration in one more dimension compared with (6) results in a counting rate of

$$N_c(\Theta_x) = A_c \int_{-\infty}^{\infty} \int_{-\infty}^{\infty} \sigma(\Theta_x m_0 c, p_y, p_z) dp_y dp_z. \quad (7)$$

The angular resolution is realized by lead slits (Fig. 7). It can be adjusted in the range 0.2 to 5 mrad. The energy resolution of a corresponding Doppler-broadening experiment would range from 0.05 to 1.3 keV. Thus, ACAR has a much better momentum resolution than the Doppler-broadening technique.

The source is placed outside the visual field of the detectors. The sample-detector distance amounts to several meters. Because of this large distance, annihilation quanta from only a small solid angle are detected. Thus, much stronger sources compared with conventional positron lifetime and Doppler-broadening measurements are required. In order to minimize the reduction of the counting rate due to the distance of several mm between sample and source, a strong magnetic field of about 1 T is usually applied to guide the positrons to the sample.

The main application of angular correlation of annihilation radiation is the study of the electron structure of the bulk and of defects. The momentum resolution is significantly higher than for Doppler-broadening spectroscopy. A two-dimensional record of the momentum distribution is favorable for comparing with theoretical calculations. 1D-ACAR machines were hardly used for semiconductors, since the intensive study of semiconductors set in when 2D-ACAR machines became available. This two-dimensional detection (Fig. 8) can be carried out with position-sensitive detectors, such as multi-wire proportional chambers or Anger cameras. The electronics of the 2D-ACAR apparatus filters the coincident events of the two detectors and stores the angular deviation from

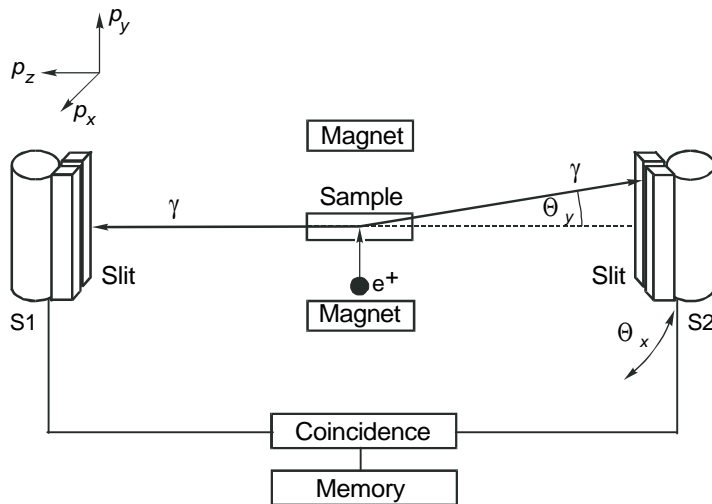


Fig. 7. Experimental setup for the measurement of one-dimensional angular correlation of annihilation radiation with a long-slit geometry. Sodium iodide crystals are used as scintillator rods (S1 and S2) in the y direction. The left arm with the detector and the lead collimators is fixed, while the right arm can be turned by the angle θ_x .

collinearity in a two-dimensional memory. No movable parts are required. The typical resolution is in the range of 0.2×0.2 mrad². The time of the measurement to collect a single 2D-ACAR spectrum amounts to several days.

In principle, the line shape parameters S and W as described in Sect. 2.2 can also be used for angular correlation of annihilation radiation. In addition, the so-called peak-height parameter H has often been used for 1D-ACAR. The measurement of this parameter can be carried out very rapidly by fixing the movable detector arm in the collinear position. However, such a parameterization as broadly applied for Doppler-broadening spectroscopy is unusual for two-dimensional angular correlation of annihilation radiation as the details of the electron structure are almost lost. The two-dimensional electron momentum distribution is contained in the whole 2D plots of the coincidence events.

As an example, the perspective and contour plots of the 2D-ACAR distribution of gallium arsenide are shown in Fig. 9 (Tanigawa et al. 1995). A four-fold symmetry with deep valleys along [001] and [010] directions is visible. Distinct maxima appear in $\langle 011 \rangle$ directions. These structures could be reproduced in first-principle calculations by Saito et al. (1991); see Fig. 10.

The electronic structure of defects can be studied in a similar way. However, in order to obtain the defect-specific plots, a normalization for saturated positron trapping, i.e. for capture of all positrons in defects, is necessary. This can be done by correlated positron lifetime measurements, which provide the fraction of positrons trapped in the defect. Such contour plots can also be directly compared with theoretical calculations to improve the understanding of the electronic structure of the defect.

The first depth-resolved measurements of the two-dimensional angular correlation of annihilation radiation were reported by Peng et al. (1996). The defect structure of the SiO₂/Si interface was studied by the combination of slow-

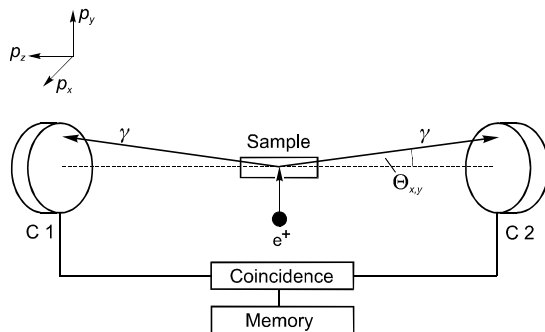


Fig. 8. Scheme of the apparatus for two-dimensional angular correlation of annihilation radiation. The angular deviation of the two γ -quanta, $\Theta_{x,y}$, is recorded by position-sensitive detectors (C1 and C2) in a coincidence setup and stored in a two-dimensional memory array.

positron-beam measurements and 2D-ACAR. The positron beam system used had a solid krypton moderator and an initial positron beam flux of about $6 \times 10^7 \text{ s}^{-1}$. The depth resolution was obtained by the variation of the incident positron energy in the range 0.2 to 20 keV. The two annihilation γ -rays were detected by position-sensitive Anger cameras located 8 m away from the sample and having an angular resolution of $1.4 \times 1.4 \text{ mrad}^2$.

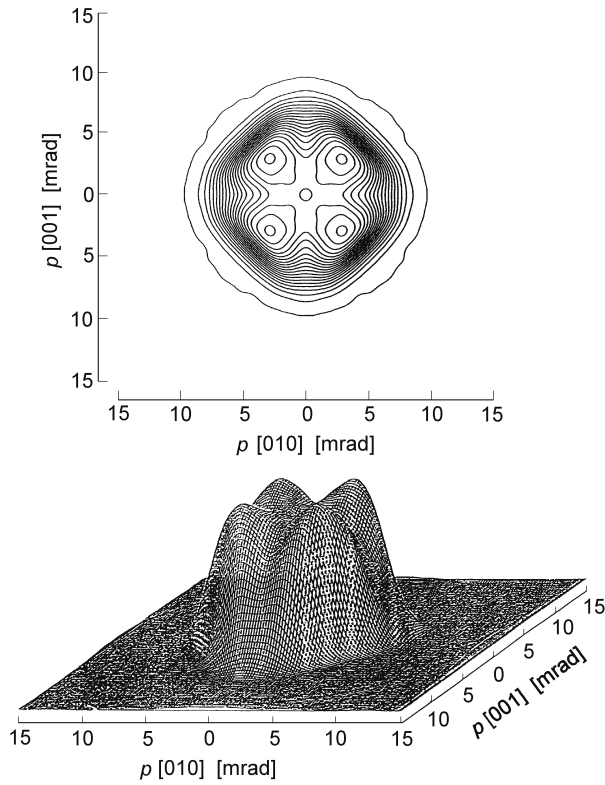


Fig. 9. Combined perspective and contour plots of the measurement of two-dimensional angular correlation of annihilation radiation in gallium arsenide exhibiting no positron trapping in defects (Tanigawa et al. 1995). The upper panel shows the contour map of the momentum distribution ρ in the (100) plane.

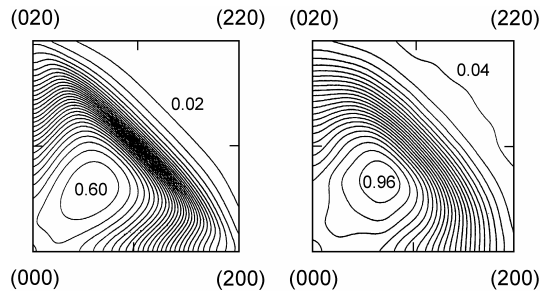


Fig. 10. Comparison of the two-dimensional angular correlation of annihilation radiation contour plot of the momentum distribution in the (001) plane of gallium arsenide obtained by ab-initio calculations (*left panel*) by Saito et al. (1991) with an experimental spectrum (*right panel*). The right panel represents a magnified part of the contour plot of Fig..